Generalized Approach toward Modeling Resist Performance

David H. Ziger and Chris A. Mack
SEMATECH, Inc., Austin, TX 78741

A generalized technique for modeling resist performance is outlined. In this approach, the fraction of resist remaining after development as a function of incident dose, or characteristic curve, is related to the development rate which is assumed to be a power law of a dominant soluble species. Soluble species are either photochemically consumed for negative resists or generated for positive. Expressions for the dependence of characteristic curves on exposure dose and chemistry are derived for various resist systems, which are consistent with current models. For similar chemical kinetics, negative resists yield fewer lumped parameters to describe their development rate and characteristic curves than positive.

Under conditions of negligible surface inhibition, lumped parameters can be extracted from characteristic curves and used to simulate lithography. A generalized method to correct for absorption in the resist and reflections is outlined. Exposure latitude was accurately predicted for a commercial negative chemically amplified resist. However, prediction of linewidths from characteristic curves of positive resists is complicated by surface inhibition effects.

Introduction

Resists are radiation-sensitive polymers which are spin-coated to form thin films and then patterned by exposure and development. Exposed regions dissolve in developer for positive acting resists, while the unexposed regions dissolve for negative resists. For overviews of lithography practices and fundamentals, see Moreau (1988) or Thompson et al. (1983). Positive and negative resists at various actinic wavelengths have been used for microlithography. For example, novolac and polyvinylphenolic resins in both tones are used extensively in microelecronics for high-resolution lithography. Since the chemistries of these systems differ, various mechanisms have been proposed to describe their lithographic behavior.

In conventional positive tone lithography, a photoactive compound (PAC) is mixed with a novolac matrix to inhibit the mixture's solubility in base. Since irradiation destroys the inhibition effect, the resist system yields a positive image of the mask after development in base. Typically, the photochemistry is modeled as first order in PAC concentration, and various models have been proposed to describe the base development (see, for example, Dill et al., 1975; Mack, 1985; Trefonas and Daniels, 1987; Hirai et al., 1987). Recently, polyvinylphenolic resins have been applied toward 248-nm and *e*-beam lithographies yielding sub 0.5-μm resolution both for positive and negative tones (Ito and Willson, 1983; Ito and Willson, 1984; Ito, 1988; Ito et al., 1990; Thackeray et al., 1989). SNR248, a negative resist (Shipley Co., Newton, MA), uses a photogenerated acid to catalyze reaction with polyvinylphenol that reduces solubility in base. Thackeray et al. (1989) have proposed that acid-catalyzed resin polymerization is the primary explanation for solubility differences in the exposed and unexposed regions. Seligson et al. (1988) and Das et al. (1990) correlated bake kinetics for these resists by proposing the effective dose concept. Fukuda and Okazaki (1990) also proposed a model based on polymerization for negative chemically-amplified resists. Furgensen et al. (1990) and Tam et al. (1990) have used FTIR and DRM techniques to measure kinetic parameters and simulate DUV lithography using the multiple-state SAMPLE model. Finally, polyvinylhydroxy-tert-butyl (t-BOC) resins have been formulated to yield positive acting high-resolution resists when combined with photogenerated acids.

Correspondence concerning this article should be addressed to D. H. Ziger, who is presently at ATT Bell Laboratories, Allentown, PA 18103.

Ito and Willson (1983, 1984) suggested that acid catalyzes decomposition of the tert-butyl functionality leaving the remaining polyvinylphenol soluble in a base such as tetramethylammonium hydroxide (TMAH). Spence and Ferguson (1991) investigated the extent of deblocking of t-BOC with FTIR techniques and postulated that the different photoacid generators can have different competing reactions during the post-exposure bake.

One problem with having specific resist models is finding general techniques to measure parameters for the lithographic models. For example, a conventional positive photoresist usually requires the Dill A B C exposure parameters and parameters for a specific develop model. Ultraviolet absorption instruments and development rate monitors (DRM) are most often used for these measurements. Development rate measurements are often tedious to obtain. Additionally, chemically amplified resists require their own parameters to model the post-exposure bake chemistry.

In this article, we propose general chemical models for positive and negative resists based on a common develop model which assumes that development is controlled by the concentration of a dominant soluble species. Due to the specific chemistry, the dose dependence of development rate assumes various forms depending on the tone, photochemistry, and post-exposure bake chemistry. Although parameters are determined best using development rate data, under conditions of minimal absorption and surface inhibition, these parameters can be extracted from conventional contrast curves. These curves show remaining resist thickness after develop as a function of exposure dose. PROLITH/2 (FINLE Technologies, Plano, TX) was used to analyze assumptions in the model for conventional and chemically-amplified positive and negative resists. We show a generalized method to correct these parameters for absorption and reflections. Simulated exposure latitude is compared to experimental results for a negative chemically-amplified resist. We call this approach the generalized characteristic model for Lithography (GCM).

Theory

In general, the remaining resist thickness after development, τ_N, normalized to the initial thickness, is given by:

$$\tau_N = 1 - \Delta\tau_{\text{PEB}} - \Delta\tau_{\text{DEV}} \tag{1}$$

where $\Delta\tau_{\text{PEB}}$ is the normalized thickness loss attributed to the post-exposure bake, and $\Delta\tau_{\text{DEV}}$ is the normalized thickness change due to development. Both of these contributions depend on the film composition. Since $\Delta\tau_{\text{PEB}}$ and $\Delta\tau_{\text{DEV}}$ can be readily measured, we wish to model these quantities to extract physical parameters for use in lithographic modeling. For both negative and positive aqueous developable resist systems, we model the resist as a mixture of a base soluble species, $[S]$, and an insoluble species, $[M]$.

Thickness loss during post-exposure bake, $\Delta\tau_{\text{PEB}}$, is modeled as a linear function of the extent of reaction of insoluble species into soluble (Eq. 2a) or soluble to insoluble (Eq. 2b) for positive and negative resist chemistries, respectively:

$$\Delta\tau_{\text{PEB}} = \Delta\tau_{(E=0)} + \left(\frac{[S]}{[M_0]}\right) G \tag{2a}$$

$$\Delta\tau_{\text{PEB}} = \Delta\tau_{(E=0)} + \left(1 - \frac{[S]}{[S_0]}\right) G \tag{2b}$$

Here $\Delta\tau_{(E=0)}$ is the thickness loss due to PEB at zero-exposure energy, and G is the fractional volume change for complete conversion. (Note that G is negligible for conventional diazonaphthoquinone systems but can be substantial for other resist chemistries. Also, $[S]$ is derived for various examples later in this section.)

We derive expressions for $\Delta\tau_{\text{DEV}}$ from the generalized rate of thickness loss during development:

$$\Delta\tau_{\text{DEV}} = \frac{\int_0^{t_{\text{DEV}}} r_{\text{DEV}}\, dt}{D} \tag{3}$$

where r_{DEV} is the development rate at time t, D is the initial resist thickness, and t_{DEV} is the development time. We assume that the development rate is proportional to the concentration of the relevant soluble species raised to a power of n:

$$r_{\text{DEV}} = k_{\text{DEV}}[S]^n \tag{4}$$

where n is a coordination number for the average number of base soluble groups that act in concert to affect solubility rate. Larger values of n imply more interaction between neighboring $[S]$ groups. In the absence of surface inhibition, absorption and standing wave effects (see the Discussion section), r_{DEV} may be considered independent of film thickness. In that case:

$$\Delta\tau_{\text{DEV}} = \frac{r_{\text{DEV}} t_{\text{DEV}}}{D} = \frac{k_{\text{DEV}} t_{\text{DEV}} [S]^n}{D} \tag{5}$$

Both $\Delta\tau_{\text{DEV}}$ and $\Delta\tau_{\text{PEB}}$ depend on $[S]$. In the following sections, $[S]$ is derived for both conventional positive diazonaphthoquinone resists and chemically-amplified positive and negative base developable systems.

Positive DNQ resists

For conventional positive DNQ resists, exposure at actinic radiation decomposes a diazonapthoquinone moiety to an indene carboxylic acid that destroys the base bulk inhibition effect. Therefore, $[S]$ is the concentration of carboxylic acid groups.

Assuming first-order photochemistry, we derive the concentration of carboxylic acid groups (which are assumed to be proportional to the concentration of deblocked novolac).

$$\frac{d[S]}{dE} = k_{\text{photo}}([M_0] - [S]) \tag{6}$$

where $[M_0] = [S] + [M]$ is the initial PAC concentration, E is the exposure energy at a particular point in the resist film, and k_{photo} is the exposure rate constant (equivalent to the Dill C parameter, Dill et al., 1975). Assuming no absorption, bleaching, or reflections, E becomes the incident energy. Integrating Eq. 6:

$$[S] = [M_0](1 - e^{-k_{photo}E}) \tag{7}$$

Substituting into Eq. 1 and Eq. 5 yields:

$$\tau_N = 1 - \Delta\tau_{PEB} - \frac{k_{DEV}t_{DEV}[M_0]^n}{D}(1 - e^{-k_{photo}E})^n \tag{8}$$

The clearing dose, E_0, is defined as the dose at which τ_N is just 0. Consequently, we can solve Eq. 8 for $(k_{DEV}t_{DEV}[M_0]^n)/D$ in terms of E_0 to obtain τ_N and r_{DEV}, respectively:

$$\tau_N = 1 - \Delta\tau_{PEB} - (1 - \Delta\tau_{PEB,E_0})\left(\frac{1 - e^{-k_{photo}E}}{1 - e^{-k_{photo}E_0}}\right)^n \tag{9a}$$

$$r_{DEV} = R_{max}(1 - e^{-k_{photo}E})^n \tag{9b}$$

where

$$\Delta\tau_{PEB} = \Delta\tau_{(E=0)} + (1 - e^{-k_{photo}E})G$$

$$E_0 = -\frac{\ln\left[1 - \left(\frac{(1 - \Delta\tau_{PEB,E_0})D}{k_{DEV}t_{DEV}[M_0]^n}\right)^{1/n}\right]}{k_{photo}}$$

$$R_{MAX} = \left(\frac{D}{t_{DEV}}\right)\frac{(1 - \Delta\tau_{PEB,E_0})}{(1 - e^{-k_{photo}E_0})^n}$$

and $\Delta\tau_{PEB,E_0}$ refers to the thickness loss after post-exposure bake at $E = E_0$ and R_{max} is a constant that can be calculated from parameters regressed from the characteristic curve. Equation 9a relates the normalized thickness as a function of exposure dose to the chemistry and develop conditions in the bulk resist. Note that R_{max} and n are intensive properties of the resist only. Once determined, r_{DEV} can be modeled for any resist thickness on any substrate. If $\Delta\tau_{PEB}$ is negligible, then Eq. 9a simplifies to:

$$\tau_N = 1 - \left(\frac{1 - e^{-k_{photo}E}}{1 - e^{-k_{photo}E_0}}\right)^n \tag{10}$$

Equation 10 was derived by Trefonas and Daniels (1987) based on polyphotolysis studies where n was related to the number of PAC groups attached to each ballast molecule.

Negative chemically-amplified resists

Photolysis for negative chemically-amplified resists generates H^+ that catalyzes a base insolublization reaction. The base soluble species, [S], for these resists is, therefore, the unreacted base soluble polymer (such as, polyvinylphenol) prior to development. Assuming the host polymer reacts via acid catalysis, we obtain [S] from the extent of reaction for the postexposure bake (PEB) process:

$$\frac{d[S]}{dt_{PEB}} = -k_{PEB}[S][H^+] \tag{11}$$

where t_{PEB} is the post-exposure bake time, $[H^+]$ is the photoacid concentration, and k_{PEB} is the rate constant.

If acid loss via side reaction (that is, termination) and diffusion are minimal, then $[H^+]$ can be assumed to stay constant during the post-exposure bake. Integrating this pseudo-first-order reaction yields:

$$[S] = [S_0]e^{-k_{PEB}[H^+]t_{PEB}} \tag{12}$$

The photoacid generator decomposes upon radiation to form protons ($PAG \xrightarrow{h\nu} H^+$). Assuming first-order decomposition photochemistry:

$$\frac{d[PAG]}{dE} = -k_{photo}[PAG] \tag{13}$$

Integrating yields:

$$[PAG] = [PAG_0]e^{-k_{photo}E} \tag{14}$$

where $[PAG_0]$ is the initial PAG concentration. Acid catalysis is sensitive to residual amine contaminants. For a given amine concentration in the photoresist, an equal amount of acid will be consumed in the neutralization reaction. Thus, the actual acid concentration will be $[H^+] = [PAG_0] - [PAG] - [amines]$. We can relate [amines] to an effective inhibition dose, E_{inhib}, which is required to generate enough acid to neutralize the amines. From Eq. 14, $[amines] = [PAG_0](1 - e^{-k_{photo}E_{inhib}})$. Thus, the acid concentration which is available to catalyze the base insolublilizing reaction will be:

$$[H^+] = [PAG_0](e^{-k_{photo}E_{inhib}})[1 - e^{-k_{photo}(E - E_{inhib})}] \tag{15}$$

Substituting Eq. 15 into Eq. 12 yields the concentration of [S]:

$$[S] = [S_0]e^{-[PAG_0]e^{-k_{photo}E_{inhib}}k_{PEB}t_{PEB}[1 - e^{-k_{photo}(E - E_{inhib})}]} \tag{16}$$

Combining Eqs. 16, 5 and 1 yields the complete normalized thickness curve:

$$\tau_N = 1 - \Delta\tau_{PEB} - \frac{k_{DEV}t_{DEV}[S_0]^n}{D}\{e^{-\alpha n e^{-k_{photo}E_{inhib}}[1 - e^{-k_{photo}(E - E_{inhib})}]}\} \tag{17}$$

where

$$\alpha = [PAG_0]k_{PEB}t_{PEB}$$

At $E = E_0$, $\tau_N = 0$. Consequently, we can solve for $(k_{DEV}t_{DEV}[S_0]^n/D)$ in terms of E_0 and substitute back into Eq. 17:

$$\tau_N = 1 - \Delta\tau_{PEB} - (1 - \Delta\tau_{PEB,E_0})e^{-\alpha n(e^{-k_{photo}E_0} - e^{-k_{photo}E})} \tag{18a}$$

$$r_{DEV} = R_{max}e^{-\alpha n(1 - e^{-k_{photo}E})} \tag{18b}$$

where

$$\Delta\tau_{PEB} = \Delta\tau_{(E=0)} + \{1 - e^{-\alpha e^{-k_{photo}E_{inhib}}[1 - e^{-k_{photo}(E - E_{inhib})}]}\}G$$

$$E_0 = E_{\text{inhib}} - \frac{1}{k_{\text{photo}}} \ln \left\{ 1 + \frac{\ln\left[\dfrac{D(1-\Delta\tau_{\text{PEB},E_0})}{k_{\text{DEV}} t_{\text{DEV}} [S_0]^n}\right]}{\alpha n e^{-k_{\text{photo}} E_{\text{inhib}}}} \right\}$$

$$R_{\max} = \frac{D}{t_{\text{DEV}}} (1 - \Delta\tau_{\text{PEB},E_0}) e^{-\alpha n (e^{-k_{\text{photo}} E_0} - 1)}$$

Note that $R_{\max}$ is obtained by solving Eq. 18b for the maximum develop rate that occurs at $E = 0$ for negative resists. As before, $R_{\max}$ is intrinsic properties of the resist. As a special case of Eq. 18a, we consider when $e^{-k_{\text{photo}} E} \approx 1 - k_{\text{photo}} E$, $E_{\text{inhib}} \approx 0$, and $\Delta\tau_{\text{PEB}} \approx 0$. In this event, Eq. 18a simplifies to:

$$\tau_N = 1 - e^{-\alpha n k_{\text{photo}} (E - E_0)} \tag{19}$$

where

$$E_0 = \frac{\ln(k_{\text{DEV}} t_{\text{DEV}} [S_0]^n / D)}{k_{\text{photo}} \alpha n}$$

Positive chemically-amplified resists

Irradiation generates acid for positive chemically-amplified resists as with negative acid hardened resists. In one positive application, the acid content cleaves a t-BOC protecting group from the polyvinylphenol host polymer during the post-exposure bake leaving polyvinylphenol, which is soluble in base. Consequently, $[S]$ is the concentration of polyvinylphenol after post-exposure bake, while $[M]$ is the concentration of the blocked functionality. We derive $[S]$ from the relevant chemical kinetics:

$$\frac{d[S]}{dt_{\text{PEB}}} = k_{\text{PEB}} ([M_0] - [S])[H^+] \tag{20}$$

Integrating Eq. 20. yields:

$$[S] = [M_0](1 - e^{-k_{\text{PEB}} [H^+] t_{\text{PEB}}}) \tag{21}$$

where the post-exposure bake is again pseudo-first order, since $[H^+]$ functions as a catalyst. We obtain $[H^+]$ from the photolysis as for negative chemically-amplified resists and derive an expression for $[S]$:

$$[S] = [M_0]\{1 - e^{-[\text{PAG}_0] e^{-k_{\text{photo}} E_{\text{inhib}}} k_{\text{PEB}} t_{\text{PEB}} [1 - e^{-k_{\text{photo}} (E - E_{\text{inhib}})}]}\} \tag{22}$$

Substituting Eq. 22 into Eqs. 5 and 1, and solving in terms of E_0 as before yields:

$$\tau_N = 1 - \Delta\tau_{\text{PEB}} - [1 - \Delta\tau_{(\text{PEB},E_0)}] \left[\frac{\{1 - e^{-\alpha e^{-k_{\text{photo}} E_{\text{inhib}}} [1 - e^{-k_{\text{photo}} (E - E_{\text{inhib}})}]}\}}{\{1 - e^{-\alpha e^{-k_{\text{photo}} E_{\text{inhib}}} [1 - e^{-k_{\text{photo}} (E_0 - E_{\text{inhib}})}]}\}} \right]^n \tag{23a}$$

$$r_{\text{DEV}} = R_{\max} \{1 - e^{-\alpha e^{-k_{\text{photo}} E_{\text{inhib}}} [1 - e^{-k_{\text{photo}} (E - E_{\text{inhib}})}]}\}^n \tag{23b}$$

where

$$\Delta\tau_{\text{PEB}} = \Delta\tau_{(E=0)} + \{1 - e^{-\alpha e^{-k_{\text{photo}} E_{\text{inhib}}} [1 - e^{-k_{\text{photo}} (E - E_{\text{inhib}})}]}\} G$$

$$E_0 = E_{\text{inhib}} - \frac{1}{k_{\text{photo}}} \ln \left[\frac{\ln\left\{1 - \left[\dfrac{(1 - \Delta\tau_{\text{PEB},E_0}) D}{(k_{\text{DEV}} t_{\text{DEV}} [M_0]^n)}\right]^{1/n}\right\}}{1 + \alpha e^{-k_{\text{photo}} E_{\text{inhib}}}} \right]$$

$$R_{\max} = \frac{D}{t_{\text{DEV}}} \frac{[1 - \Delta\tau_{(\text{PEB},E_0)}]}{\{1 - e^{-\alpha e^{-k_{\text{photo}} E_{\text{inhib}}} [1 - e^{-k_{\text{photo}} (E_0 - E_{\text{inhib}})}]}\}^n}$$

and α is defined as before.

As a special case of Eq. 23a, consider when $1 - e^{-k_{\text{photo}} (E - E_{\text{inhib}})} \approx k_{\text{photo}} (E - E_{\text{inhib}})$, $E_{\text{inhib}} \approx 0$, and $\Delta\tau_{\text{PEB}} \approx 0$. In this case, we obtain:

$$\tau_N = 1 - \left[\frac{(1 - e^{-\alpha k_{\text{photo}} E})}{(1 - e^{-\alpha k_{\text{photo}} E_0})} \right]^n \tag{24}$$

Note that Eq. 24 assumes the same mathematical form as conventional positive photoresists (Eq. 10) where α effectively amplifies the dose.

Experimental Studies

Results predicted by the generalized approach outlined in the last section were investigated by two techniques.

First, computer simulations were used to investigate extracting lumped parameters from the characteristic curves and using these parameters for lithographic modeling. PROLITH/2 (FINLE Technologies, Plano, TX) is a lithographic simulation program that can model effects of resist absorption, bleaching, and nonuniform development rates on developed linewidths and characteristic curves. These effects are neglected in the GCM approach. Consequently, by comparing parameters used to simulate τ_N and those extracted, we can measure and correct the effect of GCM assumptions on lithographic simulation.

For conventional positive resists, we wanted to determine the effect of nonuniform development rates on the accuracy of GCM simulation. In particular, inhibition effects can drastically affect the characteristic curve (Mack, 1991). Characteristic curves were simulated for conventional positive photoresist for conditions that varied the ratio of the dissolution rate at the surface to the bulk (r_s) from 1 to 0.001. For these simulations, we assumed a hypothetical resist on a nonreflecting substrate, in which bleaching, absorption, and resist shrinkage during PEB were negligible. Table 1 summarizes the resist and develop parameters that were used in the PROLITH/2 simulation.

Surface inhibition is not observed with negative chemically-amplified resists (see Discussion). Simulations of these resists were done to quantify the effect that absorption and reflections have on the accuracy of GCM parameters (that is, αn and E_0) extracted from characteristic curves. Consequently, we wanted to simulate characteristic curves for a negative resist with optical properties similar to SNR248, extract αn and E_0, and compare these values to the simulation inputs.

The method used was as follows. We varied inputs to PROLITH/2 over a wide range, and characteristic curves were then simulated for a particular resist (see Table 2, optical parameters

Table 1. Positive Resist Exposure and Development Parameters for PROLITH/2 Simulations*

Parameter	Value
A (μm^{-1})	0
B (μm^{-1})	0
k_{photo} (cm^2/mJ)	0.015
Refractive Index	1.0
Resist Thickness, D (μm)	1.0
t_{DEV} (s)	90
R_{max} (nm/s)	100
R_{min} (nm/s)	0
n	5
M_{th}	−100
Inhibition Depth (μm)	0.1
r_s	1, 0.1, 0.001

* Develop parameters are for the model discussed by Mack (1985).

are those for SNR248). Since PROLITH/2 accounts for bleaching, absorption, and reflections, r_{DEV} will vary with depth into the resist, which will affect the simulated characteristic curve. The simulated curve is then fit according to the GCM expression for τ_N (Eq. 18a with $\Delta\tau_{PEB} = 0$). By comparing values of the inputs to PROLITH/2 vs. those extracted from simulated curves, we can quantitatively correct for absorption and reflection in a self-consistent manner for a resist. The corrected parameters are independent of the substrate and depend only on the resist and development conditions. Note that this procedure must be repeated if the optical parameters differ from those shown in Table 2.

To verify the GCM approach for a negative chemically-amplified resist, characteristic curves and linewidths were measured for SNR248 resist using the test pattern shown in Figure 1. A pattern of increasing exposures was interwound with a serpentine of resolution die (See Figure 1). In this manner, simulations using parameters extracted from the GCM model could be directly compared to resolved images under the same conditions that were used to generate the characteristic curves. Partial resist thicknesses were measured using an FT500 (Prometrix, Santa Clara, CA) interferometric thickness measuring instrument. The effect of uncertainty in the optical parameters on absolute resist thickness was minimized, because only relative differences ($\Delta\tau_{PEB}$ and $\Delta\tau_{DEV}$) were analyzed. All exposures were done on a 0.35NA GCA Laserstep Stepper (GCA Corp., Andover, MA) operating at 248 nm. An organic antireflection coating, DUV-3 (Brewer Science, Rolla, MO),

Table 2. Parameters for PROLITH/2 Simulation of a Negative Chemically-Amplified Resist*

Parameter	Value
A (μm^{-1})	−1.1
B (μm^{-1})	0.7
k_{photo} (cm^2/mJ)	0.004
Refractive Index	1.8
t_{DEV} (s)	90
αn	45–210
R_{max} (nm/s)	50–500**
R_{min} (nm/s)	0.2
M_{th}	−100

* Develop parameters are for the model discussed by Mack (1985).
** This has the effect of varying E_0 from 2 to 16 mJ/cm^2.

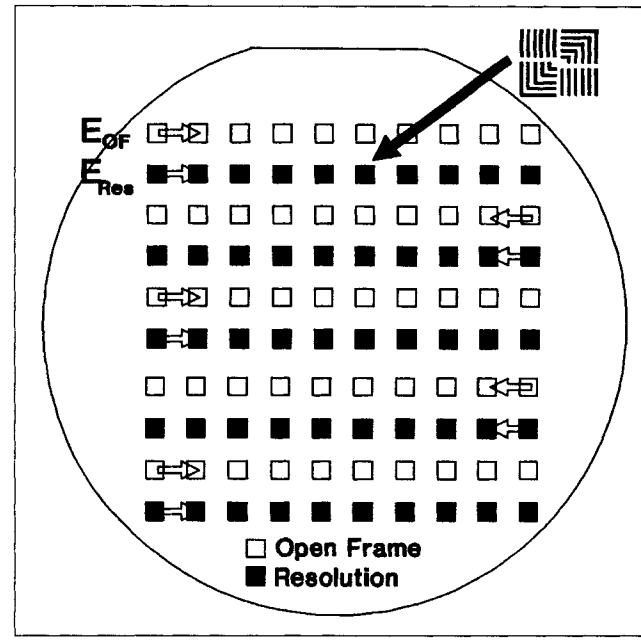

Figure 1. Two-pass test structure.
Characteristic curves and linewidth measurements could be obtained on the same wafer.

was used under the SNR248 resist to eliminate reflections at the actinic wavelength. DUV-3 does not interfere with the FT500 interferometric resist thickness measurements, because the coating is very transparent (absorption < 0.05) at the wavelengths used for measurement (400–800 nm).

Since we use a self-consistent method to correct for absorption and reflections, the purpose of antireflection coating under the resist is basically to reduce the experimental error in measuring the GCM parameters. By eliminating substrate reflections, four sources of experimental error are reduced. First, substrate reflections cause the energy coupled into the resist to depend strongly on resist thickness. Therefore, local resist thickness variations may cause significant experimental error in the measurement of characteristic curves on reflecting substrates. This is especially true in the DUV (248 nm), in which resist thickness variations of 0.02 μm on reflecting substrates can cause the energy coupled into the resist to change by about 100%. Second, the substrate optical parameters may not be accurately known, and diffuse reflectance, if present, would cause additional error in the calculated energy distribution in the photoresist. Third, reflections could cause a staircase effect in the characteristic curve if a post-exposure bake does not average out the standing waves. GCM will fit an average curve through the staircase but at the expense of additional error.

A final error is that standing waves can exaggerate surface effects, especially in positive resist systems. This happens if a standing wave node should occur at the resist surface. In that event, development rate will be a minimum at the surface that exaggerates surface inhibition effects. In general, it is better to accurately measure the lumped parameters on nonreflecting film stacks (that is, antireflection coating on silicon) and use the results to evaluate r_{DEV} that can then be used to simulate general cases. Once we correct the extracted parameters for absorption and reflections, the resulting parameters can be

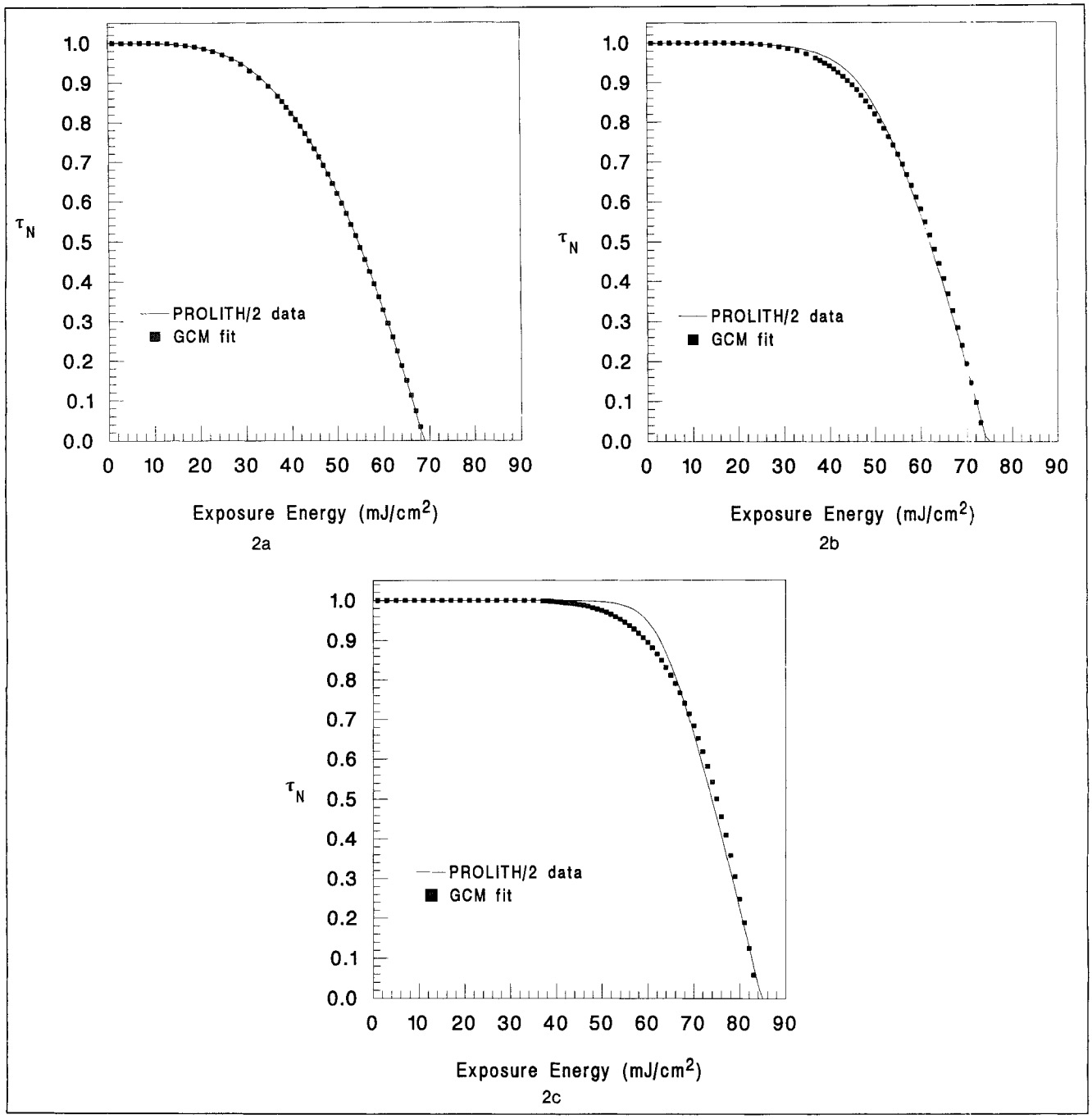

Figure 2. Characteristic curves simulated with PROLITH/2 and fitted with the GCM model for varying surface inhibition effects.

The top 0.1-μm dissolves a) the same ($r_s = 1$), b) 0.1 ($r_s = 0.1$), and c) 0.001 ($r_s = 0.001$) times as fast as the bulk.

used to simulate lithography on any stack, provided the optical parameters are known sufficiently well.

Results

Simulation

Figures 2a–2c shows PROLITH/2 simulations of a positive nonabsorbing photoresist with varying surface inhibition effects. These simulations were fit according to Eq. 10, and the parameters n and E_0 were extracted. Table 3 summarizes these results. Note that both n and the lack of fit increase as the ratio of surface to bulk development rate, r_s, decreases. In an extreme case in which $r_s = 0.001$, the value of n extracted from the characteristic curve is more than twice that used to simulate the curve. In general, as discussed later, this implies that the surface inhibition effect confounds the estimation of n from characteristic curve data.

Negative chemically-amplified resists were simulated to

Table 3. Effect of Surface Inhibition on GCM Parameter Extraction for a Conventional Positive Photoresist

		r_s		
		1.0	0.1	0.001
E_0 (mJ/cm^2)	Simulation	89.0	75	85
	Extracted	88.9	73.9	83.8
n	Simulation	5.0	5.0	5.0
	Extraction	4.9	7.2	12.0

quantify the effect that absorption and reflection have on the accuracy of extracted αn and E_0 parameters using the self-consistent approach described in the previous section. The chemical amplification and development rate models used in PROLITH/2 are quite similar to the models used in the GCM (Mack et al., 1991). Parameters α and n are direct inputs into PROLITH/2, while the development rate model requires that the maximum development rate, R_{max} (see Eq. 18b), be specified.

In the ideal case of no absorption, bleaching or reflectivity, the energy deposited in the photoresist film is equal to the incident energy. In this case, specifying α, n, and R_{max} in PROLITH/2 will result in a characteristic curve that can be fit exactly by the GCM if the regression error is negligible. The extracted parameters will be the same αn and E_0 corresponding to the input values of α, n and R_{max}. (Note that the product αn controls the development rate as a function of dose. Consequently, we varied αn for all PROLITH/2 simulations by holding α constant and varying n.) If, however, the deposited energy and the incident energy are not equal, the values of αn and E_0 extracted from the simulated contrast curve will not match the input values. Table 4 shows the results of extracting αn and E_0 from simulated contrast curves for SNR248 over a variety of input αn and R_{max} values. Table 2 summarizes the parameters used in these simulations. We can call the value of αn used as an input to PROLITH/2 the effective αn, or αn^{eff}. Similarly, the input value of R_{max} corresponds to an effective E_0, or E_0^{eff}. It is thus possible to correlate αn^{eff} and E_0^{eff} used as inputs to the simulation with the values extracted by fitting the characteristic curves to the GCM equations. The results for the parameters shown in Table 2 and the data given in Table 4 are:

Table 4. Values of E_0 and αn from PROLITH/2 Simulated Characteristic Curves

αn^{eff}	R_{max} (nm/s)			
	50	100	300	500
Values of E_0				
45	—	16.18	—	—
90	5.68	7.63	11.54	13.36
150	3.40	4.91	6.62	7.69
210	2.42	2.88	5.20	5.97
Values of αn				
45	—	50.28	—	—
90	96.4	99.5	109.4	113.9
150	160.5	173.9	181.4	189.7
210	224.7	226.7	276.1	288.4

$$E_0^{eff} = 0.93E_0 - \frac{E_0^2}{100} \tag{25a}$$

$$\alpha n^{eff} = 1.00908\alpha n - 0.0001427E_0(\alpha n)^2 \tag{25b}$$

It should be emphasized that the correlations given by Eqs. 25-26 are valid only for a resist whose optical parameters match those shown in Table 2. However, the method shown for estimating the effect of absorption on parameters extracted using GCM is completely general.

Over the full range of data given in Table 4, the average standard deviation in predicting αn^{eff} is 1.4. This error is within the regression error for fitting αn to characteristic curve data (Ziger and Mack, 1991). The average standard deviation for fitting E_0^{eff} is 0.4 mJ/cm^2. This error is larger than typical errors for fitting characteristic curve data to Eq. 18a (typical errors are 0.05–0.1 mJ/cm^2, see Ziger and Mack, 1991). However, the effect of this error is expected to be small since it is only 1% of the typical dose required to image the resist.

Application to a negative chemically-amplified resist

Since surface inhibition is not a factor for negative chemically-amplified resists (see the Discussion section), GCM parameters (αn and E_0) were extracted from SNR248 characteristic curves over a wide range of PEB and develop conditions. Figures 3a-3c show typical τ_N, $\Delta\tau_{PEB}$, and $\Delta\tau_{DEV}$ data for SNR248. In addition, Figures 3a and 3c show fitted curves. (Note that $\Delta\tau_{PEB}$ was not fit, since the absolute change in thickness was too small.) These regressed parameters were then adjusted for absorption and reflection effects using Eqs. 25a and 25b. We have reported elsewhere that linewidths simulated with extracted αn and E_0 parameters agreed within 15% of measured values over the entire experimental range that was studied (Ziger et al., 1991). For example, Figure 4 compares the predicted and experimental exposure dependence of the photoresist profile for a wafer processed at a PEB time of 60 seconds, PEB temperature of 130°C, and developed for 90 seconds in 0.135N TMAH.

Discussions

Form of GCM expressions

The GCM approach forces τ_N and r_{DEV} to have the correct behavior at the extremes of the characteristic curves for all resist systems. At $E = E_0$, the development rate is D/t_{DEV}, which is appropriately the average development rate for the dose in which the resist just clears for positive or begins to scum for negative. Conversely, as $\tau_N \to 1$, $r_{DEV} \to 0$ for all resist systems. This condition is obviously required to pattern resist. Constraining $\tau_N = 0$ at $E = E_0$ also has the effect of lumping parameters, some of which are difficult to measure, into an easily measured quantity, E_0.

It is interesting to note that negative resists yield fewer lumped parameters than corresponding positive resist systems. For example, both positive and negative chemically-amplified resist systems were derived with similar assumptions concerning PAG chemistry and bake kinetics. Yet, for negative tone, equations for τ_N and r_{DEV} lump the post-exposure bake and develop kinetics into two parameters, αn and E_0. (Note that E_{inhib} is lumped into E_0 in this case.) It is not necessary to decompose

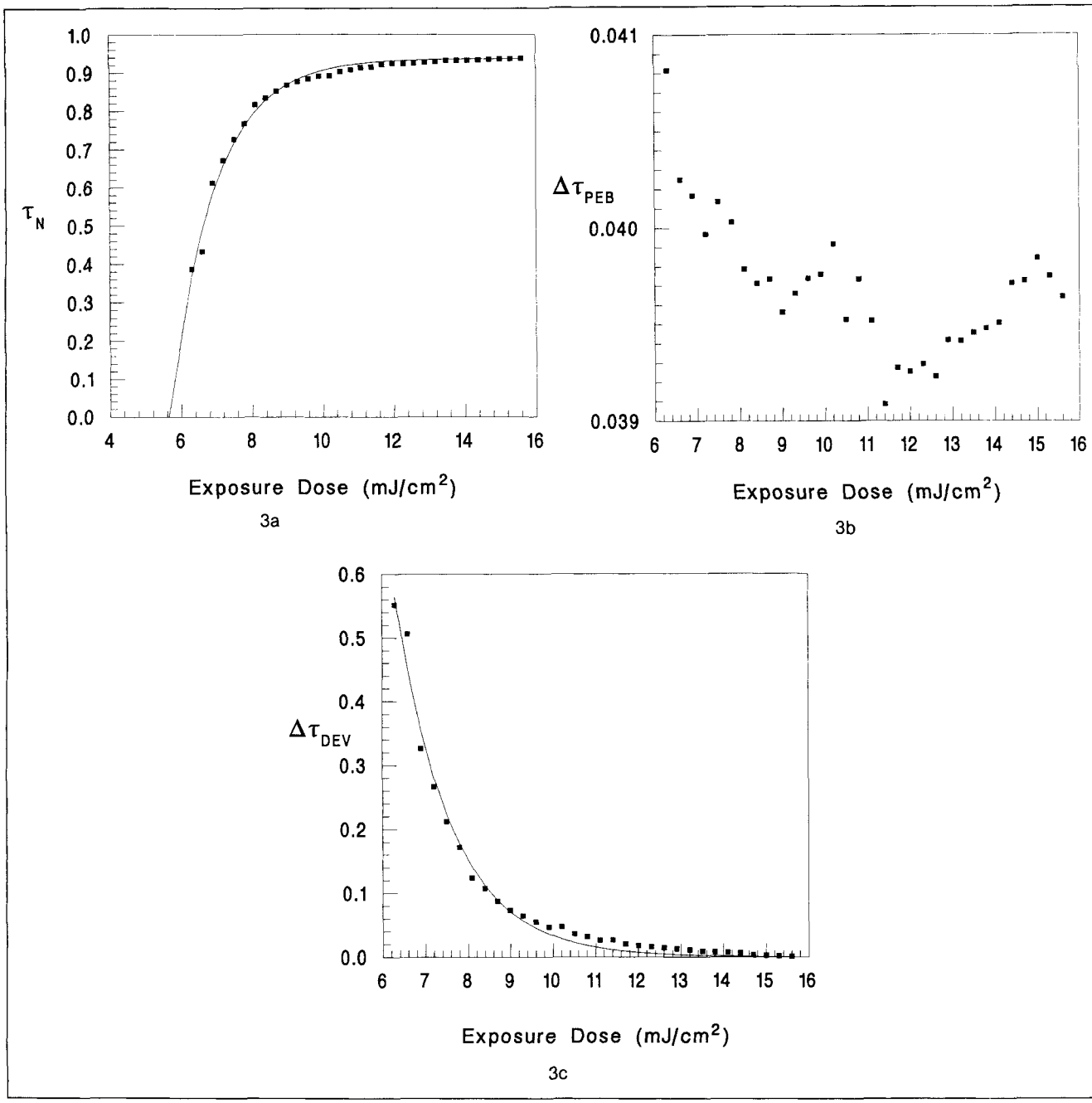

Figure 3. Experimental a) τ_N, b) $\Delta\tau_{PEB}$, and c) $\Delta\tau_{DEV}$ data for SNR248 processed at $T_{PEB} = 130°C$, $t_{PEB} = 60$ s, and $t_{DEV} = 90$ s.

GCM fitted curves shown for τ_N and $\Delta\tau_{DEV}$.

these effects to do lithographic modeling. However, the form of the positive chemically-amplified resist characteristic curve demands that the bake kinetics, α, chemical inhibition, E_{inhib}, development coordination number, n, and dose to clear, E_0, be known separately. (Perhaps, the most attractive method to do this is to accurately measure $\Delta\tau_{PEB}$ and regress these parameters. However, this is difficult to do for most lithographically-attractive materials that are designed to minimize G.). Consequently, there are only two lumped parameters (αn and E_0) for negative chemically-amplified resists, while there are as many as four (α, n, E_{inhib}, and E_0) for the positive tone.

There is a fundamental reason why negative systems yield fewer lumped parameters for the same chemistry than positive. For negative resists, [S] is proportional to an exponential function of the kinetics. Raising an exponential function to a power (to obtain r_{DEV}) lumps n together with the chemical kinetics. Meanwhile, [S] is proportional to one minus an exponential function for positive resists. Consequently, for positive resists, parameters in [S] must be known independent of n. Mathematically this leads to other simplifications for negative systems. For example, since E_{inhib} is lumped only into E_0 for negative resists, amine contaminants dissolved in the resist

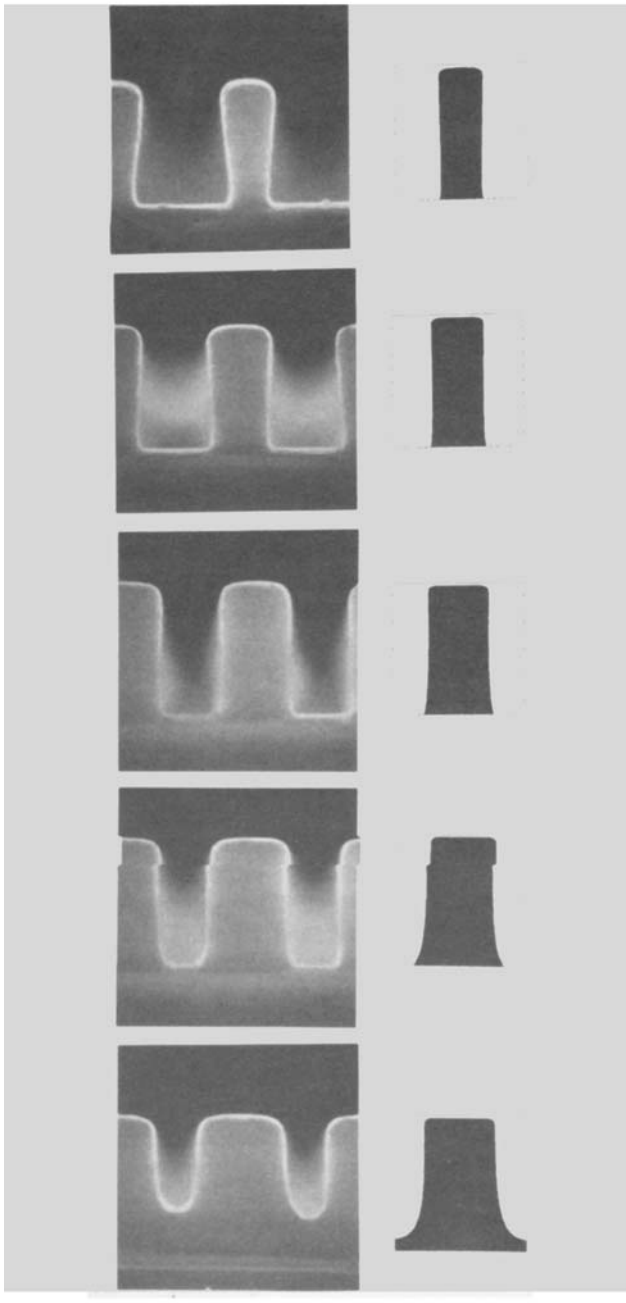

Figure 4. Simulated vs. experimental exposure latitude of 0.5-μm lines and spaces.

We used PROLITH/2 with development rate parameters extracted using the GCM approach for SNR248 negative chemically-amplified resist.

should not affect the shape of the characteristic curve. For positive chemically-amplified resists, both the shape and E_0 are expected to change with dissolved amine impurities.

It is interesting to compare expressions for τ_N for various resist systems. To simplify this comparison, we investigate the case in which we neglect post-exposure film loss ($\Delta\tau_{PEB} \approx 0$) and bulk amine contamination ($E_{inhib} \approx 0$), and assume $e^{(-k_{photo}E)} \approx 1 - k_{photo}E$. Table 5 summarizes these results. Note that the difference in expressions for τ_N is the presence of α in the chemical-amplified equations. Therefore, as a first approximation, chemical amplification is achieved only if $\alpha > 1$.

Table 5. Comparison of τ_N Expressions for Various Resist Systems*

	Conventional	Chemically Amplified
Negative**	$1 - e^{-nk_{photo}(E-E_0)}$	$1 - e^{-\alpha n k_{photo}(E-E_0)}$
Positive	$1 - \left[\frac{(1-e^{-k_{photo}E})}{1-e^{-k_{photo}E_0})}\right]^n$	$1 - \left[\frac{(1-e^{-\alpha k_{photo}E})}{1-e^{-\alpha k_{photo}E_0})}\right]^n$

* Expressions valid when: 1. $\Delta\tau_{PEB} \approx 0$; 2. $E_{inhib} \approx 0$; 3. $e^{(-k_{photo}E)} \approx 1 - k_{photo}E$.
** The expression for τ_N for a conventional negative resist is derived by a method identical to that shown in the section on Theory for other resist systems. Here, $[S]$ in Eq. 5 is assumed to be consumed by a first-order photochemical reaction with a rate constant of k_{photo}.

GCM approximations

Several approximations are contained in the GCM model. The most important of these are:

1. The development rate is a function only of a single dominant soluble species and is constant during the develop cycle.
2. The photochemistry is first order.
3. Chemically-amplified resist systems exhibit ideal catalysis with pseudo-first-order kinetics ($[H^+]$ is assumed constant).

The first assumption neglects effects that change the development rate with depth into the resist. For example, the resist surface can dissolve slower (surface inhibition) or faster (surface enhancement) than the bulk resist.

From Figures 2a–2c and Table 3, we observe that increasing surface inhibition has the effect of increasing the slope of τ_N in the vicinity of E_0. Consequently, estimation of n will be confounded by surface inhibition (Figures 2a–2c). In a similar way, surface inhibition causes resist contrast, γ, to be overestimated. Previous studies have shown that estimation of n is critical for simulating lithography, since it affects process latitude, resist sidewall angle and exposure, and focus latitude (Trefonas and Mack, 1991). Therefore, the GCM approach must be modified to compensate for surface inhibition (if possible) before it could be reliably applied toward predicting linewidths for positive resists in which surface inhibition is important.

Although surface inhibition can have a large effect on the value of αn, surface enhancement, in general, is expected to have a lesser effect. Measuring a characteristic curve has the effect of averaging development rate over the development time. By its very nature, surface inhibition increases the amount of time required to dissolve the thin inhibition layer. Thus, this slow developing region is heavily weighted in the average development rate. On the other hand, surface enhancement will cause the thin enhancement layer to be dissolved in very little time, so that it has relatively little effect on the average development rate. As a result, comparable amounts of surface inhibition and surface enhancement do not produce comparable changes in αn.

Other factors that affect the dissolution rate are absorption, bleaching, and thin-film interference effects. However, as shown in the Results section, these effects can be accounted for by correcting the extracted parameters as shown in the previous section for negative chemically-amplified resists. A

key point of this correction approach is that it is totally self-consistent. A primary parameter model is used to simulate these effects, and extracted parameters are compared with those entered into the simulation. The accuracy of the correction depends on the accuracy of the primary model (in this case, PROLITH/2) to predict these optical effects.

The assumption that development rate is a power function of a single soluble species is consistent with prior investigations and agrees with available development rate data (see, for example, Trefonas et al., 1987; Trefonas and Mack, 1991; Ferguson et al., 1990). The assumption for first-order photochemistry has been justified for conventional positive photoresist systems and is used in other simulation programs (see, for example, Dill et al., 1975). Data for the photochemical decomposition of photo acid generators have not been published.

The assumption of ideal acid catalysis in the GCM model has been discussed elsewhere (Ziger et al., 1991). Basically, indirect evidence suggests that a quenching mechanism may be important at elevated temperatures or extended postexposure bake times. The GCM model predicts αn to have an Arrhenius temperature and linear PEB time dependence. Ziger et al. (1991) measured αn over a range from 110–160°C and observed that αn saturates as a function of both PEB temperature and time. This suggests that either quenching becomes important at higher acid concentrations or that the acid catalyzed reaction becomes diffusion-limited. (Another possibility is that the power dependence on solubility is temperature-dependent above a threshold value.)

The assumption of ideal acid catalysis also implies that $[H^+]$ is locally constant, that is, diffusion is negligible. In fact, diffusion is not negligible under normal lithographic conditions. The more rigorous approach is to simultaneously solve the reaction and diffusion equations (Barouch et al., 1991). PROLITH/2 makes a simplification that diffusion occurs first and then the reaction. The GCM approach neglects diffusion, since its assumption of constant r_{DEV} implies that $[H^+]$ does not vary with position within the resist. This situation is physically reasonable for very large exposed areas on an antireflection film. Consequently, kinetic parameters can be extracted using the GCM approach and used in more rigorous models that take into account diffusion.

Development rate expressions

The development rate model proposed here for all photoresist systems ($r_{DEV} \propto [S]^n$) has been previously applied to describe conventional novolac resist systems. Mack (1985) derived the following expression:

$$r_{DEV} = R_{max} \frac{(a+1)(1-m)^n}{a+(1-m)^n} + R_{min} \tag{26}$$

where

$$a = \frac{(n+1)}{(n-1)}(1-M_{th})^n$$

For many resist systems, $M_{th} < 0$, so that Eq. 26 simplifies to:

$$r_{DEV} = R_{max}(1-m)^n + R_{min} \tag{27}$$

Since $[1-m]$ is the relative concentration of the base soluble carboxylic acid, the GCM develop model is consistent with Mack's model, provided R_{min} is negligible. Development rate expressions equivalent to Eq. 27 have been proposed by Trefonas and Daniels (1987) and Hirai et al. (1987). Lastly, it should be noted that R_{min} can be accounted for in the GCM approach by measuring the thickness loss of regions exposed at very large doses for negative resists and at zero dose for positive resists. The effect of R_{min} on τ_N can then be lumped into $\Delta\tau_{PEB}$. For SNR248, R_{min} was about 0.23 nm/s.

Furguson and coworkers (1990) used a similar functional form for r_{DEV} to model negative DUV resists:

$$r_{DEV} = R_0 \left[1 - \frac{CE_{(CS)}}{C_0}\right]^a \tag{28}$$

where R_0, C_0, and a are regressed from development rate data, and $CE_{(CS)}$ is obtained from acid catalyzed cross-linking kinetics. If $[1 - CE_{(CS)}/C_0]$ is an effective soluble species concentration, then this model is equivalent to the one adopted for the GCM approach.

Comparison with other approaches

It is interesting to compare GCM assumptions and results with other models.

Equations relating the PAC decomposition with exposure dose used in the GCM model for positive photoresists were derived by Dill and coworkers (1975) and are used in simulation programs such as SAMPLE and PROLITH/2. Neglecting thickness loss due to post-exposure baking, Trefonas and Daniels previously derived the expression for τ_N (Eq. 10), though the dependence of E_0 on processing conditions and formulation was not explicitly stated.

As stated in the Introduction, the conventional approach toward modeling acid catalyzed negative resists has been to formulate the kinetics of polymerization. Development rate parameters are regressed from DRM data that are then correlated to FTIR data.

The generalized characteristic model for lithography is a consistent approach toward modeling resist performance that provides an outline for characterizing resists, whether positive or negative, conventional or chemically-amplified. Consequently, an advantage of the GCM approach is that it provides a framework for understanding the similarities and differences between positive and negative resists of complimentary chemistries.

Linewidth simulations

For SNR248, we have reported elsewhere (Ziger et al., 1991) that the αn and E_0 parameters extracted from characteristic curves were used to simulate linewidths within 15% of experimental values over a range of postexposure bake temperatures and times from 110–150°C and 30–90s, respectively, and develop times from 30–150s. Figure 4 shows that exposure latitude was accurately predicted (Mack et al., 1991). Consequently, the GCM approach is a viable predictor of lithographic response over essentially the entire operating range

of this resist. Furthermore, this technique is expected to work well for any negative chemically amplified resist system primarily because of the lack of surface inhibition in these systems.

As mentioned earlier, E_0 and αn parameters can be corrected for both absorption and substrate effects. A rigorous test of this is to measure the development parameters on one substrate to predict linewidths on another. Figure 5 shows experimental and predicted linewidths for resist on silicon. The r_{DEV} parameters were obtained from a characteristic curve of resist on DUV-3 antireflecting coating and subsequently corrected for absorption using Eqs. 25a-25b. Note that both experiment and theory predict stepper sidewall profiles. This is due to substrate reflections. Agreement between experiment and simulated linewidths was within 14%.

Additional work

A challenging problem is to determine under what conditions the GCM approach can be used to extract meaningful kinetic parameters for positive resists from τ_N. We have shown that surface inhibition confounds estimation of bulk dissolution properties from τ_N. However, there could be ways to estimate the inhibition effect from the lack of fit of the GCM model with characteristic curve data for several develop times.

Conclusions

The generalized characterization model for Lithography is a generalized approach toward modeling resist performance. Characteristic curves for positive and negative conventional and chemically-amplified resists can be modeled using consistent assumptions. Positive systems usually require more lumped parameters to model characteristic curves and development rates than negative. In the absence of surface inhibition, lumped parameters can be extracted from characteristic curves to accurately model development rates as a function of dose. Simulation programs can then be used to predict linewidths. This technique was applied to negative chemically-amplified resists to successfully predict linewidths and process latitudes.

Acknowledgment

The authors wish to acknowledge the following individuals at SEMATECH for their contributions: Romelia Distasio for experimental work and Orlando Castanon for SEM work. Discussions with Dr. Charles Szmanda and Dr. Jim Thackeray (Shipley Co.) concerning SNR248 chemistry were instrumental toward the development of the GCM approach. We also acknowledge useful conversations with Dr. Richard Ferguson, Prof. Andrew Neureuther and Prof. William Oldham (University of California, Berkeley), and Prof. Eytan Barouch (Princeton University) and Dr. Daniel Seligson (Intel).

Notation

A,B = Dill model (1975) exposure parameters
D = resist thickness prior to exposure
E = dose in the resist
E_0 = dose at which the resist clears for positive resist and begins scumming for negative
E_{inhib} = effective dose required to generate protons to neutralize basic contaminants
E_0^{eff} = effective E_0 compensating for absorption
G = fractional resist thickness of volume change for complete conversion after PEB

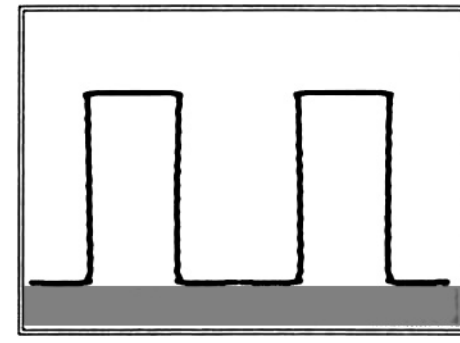

(a)

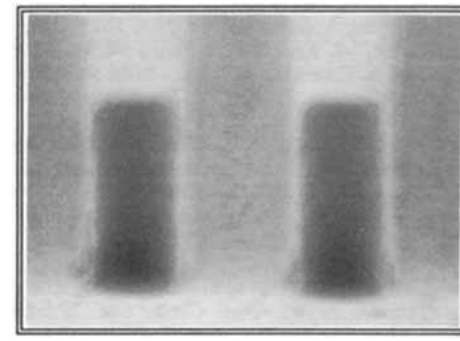

(b)

Figure 5. (a) Simulated vs. (b) experimental linewidths for SNR248 for nominal 0.5-μm dense lines on silicon.

Development rate parameters were obtained from a characteristic curve on a nonreflecting substrate.

H^+ = protons (generated from PAG)
k_{DEV} = rate constant for development
k_{PEB} = rate constant for post-exposure bake
k_{photo} = rate constant for photochemistry
M = base insoluble species
S = base soluble species
n = dissolution rate power
PAC = photoactive compound (diazonaphthoquinone)
PAG = photoacid generator
r_{DEV} = development rate
r_s = ratio of surface to bulk development rates
R_{max}, R_{min}, M_{th} = Mack model (1985) develop rate parameters
t_{DEV} = develop time
t_{PEB} = post-exposure bake time

Greek letters

α = lumped kinetic parameter for chemically amplified resists = $[PAG_0]k_{PEB}t_{PEB}$
τ_N = final resist thickness after development normalized to D
$\Delta\tau_{DEV}$ = change in normalized resist thickness due to development

$\Delta\tau_{PEB}$ = change in normalized resist thickness due to post-exposure bake
αn^{eff} = effective value of αn compensating for absorption and reflections

Subscript

0 = initial concentration

Literature Cited

Barouch, E., B. Bradie, U. Hollerbach, G. Karniadakis, and S. Orszag, "Comprehensive 3-D Notching Simulator with Nonplanar Substrates," *Proc. SPIE*, **1264**, 334 (1990).

Das, S., and D. Seligson, "Characterization and Process Control of Thermally Activated Resists," *Proc. Int. Photopolymers Conf.*, Ellenville, NY (1988).

Das, S., J. Thackeray, M. Endo, J. Langston, and H. Gaw, "A Systematic Investigation of the Photoresponse and Dissolution Characteristics of an Acid Hardened Resist," *Proc. SPIE*, **1262**, 60 (1990).

Dill, F. H., W. P. Hornberger, P. S. Hauge, and J. M. Shaw, "Characterization of Positive Photoresist," *IEEE Trans. Electron Devices*, **ED-22**, 445 (1975).

Ferguson, R. A., J. M. Hutchinson, C. A. Spence, and A. R. Neureuther, "Modeling and Simulation of a Deep-Ultraviolet Acid Hardening Resist," *J. Vac. Sci. Technol.*, **B8**, 1423 (1990).

Fukuda, H., and S. Okazaki, "Kinetic Model and Simulation for Chemical Amplification Resists," *J. Electrochem. Soc.*, **137**, 675 (1990).

Hirai, Y., M. Sasago, M. Endo, K. Tsuj, and Y. Mano, "Process Modeling for Photoresist Development and Design of DLR/sd Process," *IEEE Trans. Computer-Aided Design*, **CAD-6**, 403 (1987).

Ito, H., and C. G. Willson, "Chemical Amplification in the Design of Dry Developing Resist Materials," *Polym. Eng. Sci.*, **23**, 1012 (1983).

Ito, H., and C. G. Willson, *Polymers in Electronics, ACS Symp. Ser.*, No. 242, T. Davidson, ed., Amer. Chem. Soc., Washington, DC, 11 (1984).

Ito, H., "Sensitive Resist Systems Based on Acid Catalysis: Chemical Amplification," *Proc. KTI Microelectronics Seminar*, 81 (1988).

Ito, H., L. A. Pederson, K. N. Chiong, S. Sonchik, and C. Tsai, "Sensitive Electron Beam Resist Systems Based on Acid-Catalyzed Deprotection," *Proc. SPIE*, **1086**, 11 (1989).

MacDonald, S. A., C. D. Snyder, N. J. Clecak, R. Went, C. G. Willson, C. J. Knors, N. B. Deyoe, J. G. Maltabes, and J. R. Morrow, "Airborne Chemical Contamination of a Chemically Amplified Resist," *Proc. SPIE*, **1466**, 2 (1991).

Mack, C. A., "PROLITH: a Comprehensive Optical Lithography Model," *Proc. SPIE*, **538**, 207 (1985).

Mack, C. A., "Lithographic Optimization Using Photoresist Contrast," *Microelectronics Mfg. Tech.*, **14**, 36 (1991).

Mack, C. A., E. Capsuto, S. Sethi, and J. Witowski, "Modeling and Characterization of a 0.5-μm-Deep Ultraviolet Process," *J. Vac. Sci. Technol. B*, in press (1991).

Moreau, W., *Semiconductor Lithography Principles, Practices and Materials*, Plenum Press, New York (1988).

Seligson, D., S. Das, H. Gaw, and P. Pianetta, "Process Control with Chemical Amplification Resists Using Deep Ultraviolet and X-Ray Radiation," *J. Vac. Sci. Technol.* **B6**, 2303 (1988).

Spence, C. A., and R. A. Ferguson, "Some Experimental Techniques for Characterizing the Performance of Photoresists," *Proc. SPIE*, **1466**, 324 (1991).

Tam, N. N., R. A. Ferguson, A. Titus, J. M. Hutchinson, C. A. Spence, and A. R. Neureuther, "Comparison of Exposure, Bake and Dissolution Characteristics of Electron Beam and Optically Exposed Chemically Amplified Resists," *J. Vac. Sci. Technol.*, **B8**, 1470 (1990).

Thackeray, J. W., G. W. Orsula, D. Canistro, E. K. Pavelcheck, L. E. Bogan, A. K. Berry, and K. A. Graziano, "DUV ANR Photoresists for 248-nm Excimer Laser Photolithography," *Proc. SPIE*, **1086**, 34 (1989).

Thompson, L. F, C. G. Willson, and M. J. Bowden, eds. *Introduction to Microlithography, ACS Symp. Ser.*, No. 219, Washington, DC (1983).

Trefonas, P., and B. K. Daniels, "New Principle for Image Enhancement in Single-Layer Positive Photoresists," *Proc. SPIE*, **771**, 194 (1987).

Trefonas, P., and C. A. Mack, "Exposure Dose Optimization for a Positive Resist Containing Poly-functional Photoactive Compound," *Proc. SPIE*, **1466**, 117 (1991).

Ziger, D., C. A. Mack, and R. Distasio, "The Generalized Characteristic Model for Lithography: Application to Negatively Chemically Amplified Resists," *Proc. SPIE*, **1466**, 270 (1991).

Manuscript received July 22, 1991, and revision received Oct 11, 1991.